A Gadolinium Spin Label with Both a Narrow Central Transition and Short Tether for use in Double Electron Electron Resonance Distance Measurements

Anokhi Shah,[†,‡] Amandine Roux,[¶] Matthieu Starck,[¶] Jackie A. Mosely,[¶] Michael Stevens,[§] David G. Norman,[§] Robert I. Hunter,[†] Hassane El Mkami,[†] Graham M. Smith,[†] David Parker,[*,¶] and Janet E. Lovett[*,†,‡]

†*SUPA, School of Physics and Astronomy, University of St Andrews, St Andrews, KY16 9SS, U.K.*
‡*BSRC, University of St Andrews, St Andrews, KY16 9ST, U.K.*
¶*Department of Chemistry, Durham University, South Road, Durham DH1 3LE, UK.*
§*College of Life Sciences, University of Dundee, Dow Street, Dundee, DD1 5EH, UK.*

Received January 30, 2019; E-mail: david.parker@durham.ac.uk; jel20@st-andrews.ac.uk

Abstract: The design, synthesis and application of a nine-coordinate gadolinium(III)-containing spin label, [Gd.sTPATCN]-SL, for use in nanometer-distance measurement experiments by EPR spectroscopy is presented. The spin label links to cysteines via a short thioether tether and has a narrow central transition indicative of small zero-field splitting (ZFS). A protein homodimer, TRIM25cc, was selectively labeled with [Gd.sTPATCN]-SL (70%) and a nitroxide (30%) under mild conditions and measured using the double electron electron resonance (DEER) technique with both commercial Q-band and home-built W-band spectrometers. The label shows great promise for increasing the sensitivity of DEER measurements through both its favorable relaxation parameters, and the large DEER modulation depth at both Q- and W-band for the inter-Gd(III) DEER measurement which, at 9%, is the largest recorded under these conditions.

INTRODUCTION

One application of EPR spectroscopy which is garnering particular interest and rapid improvement is its ability to measure nanometer-range distance measurements through the detection of the dipole-dipole coupling between either endogenous or exogenous paramagnetic centers. This is particularly useful in soft matter research including structural biology. For example a protein, or other biomolecule, may have paramagnetic centers in the form of "spin labels" placed site-specifically, which enables measurement of inter- or intra-biomolecular distances.[1] Gadolinium(III) complexes offer a range of improvements over the more frequently applied nitroxide spin labels.[2–5] For example: greater stability within biological cells, enabling the use of EPR for in-cell structural biology;[6–9] improvements in the sensitivity of measurements due to their high spin properties without adding the complication of orientation selection;[2,10] and providing a paramagnetic center with complementary magnetic properties to nitroxides, so that distance measurements may be made between selected spin labels in a multi-labeled sample, in a strategy termed "spectroscopically orthogonal" labeling.[3,11–17]

In this work we show the rational design and subsequent synthesis of a nine-coordinate Gd(III) ligand for utilization as a spin label in EPR for distance measurements. We focus on keeping the lineshape of the Gd(III) EPR spectrum narrow, which should afford better concentration sensitivity and signal-to-noise, and minimising the linker length between the Gd(III) and the biomolecule. This paper is organized as follows: first we introduce the area of Gd(III) spin labeling through a very short review of the literature with a focus on what advances may lead to increased sensitivity for distance measurements, both for signal-to-noise and accurate distance abstraction. Then we introduce the design of the label. We present its synthesis and use it to modify cysteine residues for site-directed spin labeling. Finally we use double electron electron resonance (DEER, also known as PELDOR) experiments at Q- and W-band frequencies to test a protein mixed-labeled with the new probe and with a nitroxide spin label.[18,19] We show that the label has promising features for increasing the sensitivity of the DEER experiment through increased modulation depth in DEER and increased persistence of its echo (phase memory time) compared to existing Gd(III) spin labels.

Gadolinium(III) is a paramagnetic ion with $S = \frac{7}{2}$. As such Gd(III) complexes have a significant zero-field splitting (ZFS) interaction which is characterized by two parameters D and E with values related to the symmetry of the coordination - in high symmetry D would be near 0, and $\mid E \mid \leq \mid \frac{D}{3} \mid$.[20] At Q-band (35 GHz, B_0 1.25 T) EPR frequencies and above, complexes with the smaller D values are in the high field limit, i.e. $D << g\mu_B B_0$.[17] In this case, the frozen solution (powder) EPR absorption spectrum is broad and featureless for the various transitions due to a distribution in the ZFS parameters, except for a relatively narrow central line from the $|-\frac{1}{2}\rangle \rightarrow |+\frac{1}{2}\rangle$ transition. The width of the central transition is proportional to $\frac{D^2}{gB_0}$.[2]

Gd(III)-Gd(III) distances up to 3.8 nm have been detected through the broadening of the central transition caused by unresolved dipole-dipole coupling.[21] These measurements were performed at very high microwave frequencies with continuous wave (CW) EPR. Distances between 2 and 8.6 nm have been measured using the pulsed EPR methods of DEER and relaxation induced dipolar modulation enhancement (RIDME).[18,19,22–24] The available distance range is complementary to other biophysical methods and very useful for determining biomacromolecular structure.[1,3,4]

RIDME experiments for Gd(III) centers provide an increased signal compared to DEER but measure higher order (overtone) harmonics of the dipole-dipole coupling which complicates the data analysis for providing distances and

distance distributions.[24] DEER measurements are not prone to this complication, and this study utilizes only four-pulse DEER.[18,19] The pulse sequence for this experiment uses a refocussed Hahn echo for the observer sequence at one frequency, and an inversion (pump) pulse at a second frequency.[19] By pumping spins that are dipolar coupled to the observed set at variable times through the sequence, the refocussed echo intensity is modulated at a frequency corresponding to the dipole-dipole coupling frequency. Gd(III) complexes can be treated as $S = \frac{1}{2}$ centers if the ZFS parameter D is sufficiently small and the measured frequency is proportional to the inverse cube of the distance between the paramagnetic centers.[17,25] In these conditions software such as DeerAnalysis is available to allow extraction of average distances and distributions.[26] Though an interesting new class of Gd(III) spin label is characterized as having a larger D,[27] most Gd(III) complexes used as spin labels have a ZFS D less than ∼1200 MHz.[28] Gd(III) complexes with a ZFS parameter $D < 1100$ MHz must have their pseudo-secular terms in the Hamiltonian taken into account to properly analyse DEER data corresponding to distances < 4.0 nm.[23,25] This limitation is removed if a sufficiently broad bandwidth is available such that the pump and observer frequencies in the DEER experiment are able to excite different Gd(III) transitions.[29,30] Previous studies have shown that the DEER experiment is optimized by setting the pump pulse at the top of the narrow central transition and offsetting the observer pulse sequence by an amount sufficient to ensure both a sufficiently large detected echo, no pulse overlap and, for small ZFS/short distances, ensuring the weak-coupling regime for the dipolar coupling.[2,30]

Chirped and shaped pulses, made possible through the application of arbitrary waveform generators (AWGs), provide increased sensitivity for DEER experiments at Q- and W-band (*ca.* 95 GHz, B_0 3.4 T).[31–33] However, spectrometers that operate with AWGs are not yet commonplace. In this paper, we do not use shaped pulses but instead compare results for our label through measurements using the standard 4-pulse DEER sequence with a Bruker Q-band spectrometer and "HiPER", a home-built high power kW W-band spectrometer (94 GHz, B_0 3.34 T) which offers both high sensitivity and an 800 MHz instantaneous bandwidth.[34,35] HiPER allows considerable flexibility in selecting the position of the pump and observer pulses. The spectrometer shares some common features with the PNNL EMSL instrument which was used to demonstrate the bandwidth and increased power on a Gd(III) labeled DNA sample in the Supplementary Materials of the reference.[36]

The absolute sensitivity of the DEER experiment relies on the product of the echo intensity at the observer frequency and modulation depth of the signal.[2,36,37] The echo intensity will depend upon the population of spins that can be probed and relaxation rates at that position.[36] Since the DEER experiment measures the dipole-dipole coupling that varies as the inverse-cube of the interspin distance, an increased phase memory time (T_m) will allow larger distances to be accurately determined through measurement of a longer DEER time trace.[38] The spin-lattice time (T_1) is also important since it determines how often an experiment can be repeated within a given time and thus the ability to signal average. The optimal signal-to-noise ratio is achieved through balancing the DEER measurement temperature according to T_m and T_1 values and the population of the transitions to be measured.[2] For example, for $S = \frac{1}{2}$ nitroxides, 50 K is

jel resized after round 2.png

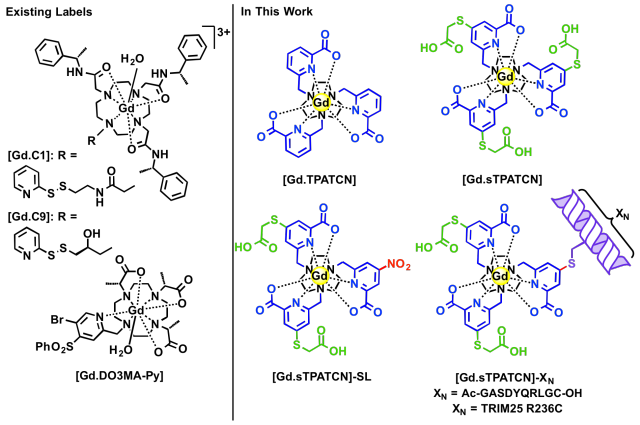

Figure 1. Chemical structures of existing Gd(III) spin labels significantly relevant to this work,[9,40,41] and the Gd(III) complexes presented in this article. X_N represents a thiol-containing biomolecule.

a good choice of temperature for DEER experiments due to the balance between long T_m and short T_1 at this temperature.[38] In contrast, the high-spin nature of Gd(III) means it is preferable to measure at a lower temperature since T_1 is short and not limiting and T_m increases as the temperature is lowered.[39] However, the population of the $|-\frac{1}{2}\rangle \rightarrow |+\frac{1}{2}\rangle$ transition eventually reduces at lower temperatures and generally a balance is found at around 10 K.[2]

The modulation depth (herein also called λ) is related to the fraction of spins excited by the pump pulse and the probability that they are inverted. It is measured experimentally as the difference from unity for the normalized form factor of the DEER time trace after the modulations have been damped, where the form factor is obtained from the primary data through background correction.[26] As it is important to maximize the fraction of pumped spins to increase sensitivity, a complex with small ZFS, and therefore a narrow central transition, is desirable. A number of Gd(III) complexes have previously been investigated. The full-width at half-height (FWHH) of the central transition for the DOTA derivative [Gd.C1] (Figure 1) is reported as 1.15 mT (95 GHz, 10 K) and this is the narrowest central transition for a spin label attached to a biomolecule so far reported.[27,30,40] However, it has a long linker, which can result in broad distance distributions. Decreasing the length between the Gd(III) and the protein, to give [Gd.C9] (Figure 1), which is desirable for precision distance measurements, increased the FWHH of the central transition to 2.48 mT (95 GHz, 10 K).[27,30,41] Both of these DOTA derived spin labels form a disulfide bond with a cysteine residue. In contrast, the [Gd.DO3MA-3BrPy] spin label (see Figure 1) has been developed to conjugate to cysteine via a thioether bond which provides the shortest linker arm to date, and - unlike a disulfide - was shown to be chemically stable for in-cell applications.[9] The FWHH of the central transition of the label was reported to be 6.4 mT (reported as 180 MHz, W-band, 10 K) which is much broader than [Gd.C1].[9] Very recent work reports that through removal of the methyl group from the methyl acetate of the ligand in [Gd.DO3MA-3BrPy] the ZFS of the Gd(III) is reduced and the phase memory time is extended, which increases the DEER experiment sensitivity.[42]

However, there is a class of Gd(III) complex that has been identified as a promising candidate for new spin la-

bels.[20] This is the nine-coordinate Gd(III) complex of the 9-N_3 tris(pyridine-2-carboxylate) ligand [Gd.TPATCN] (Figure 1).[43,44] Previous solution-state CW EPR studies indicate that it has a small peak-to-peak linewidth (a parameter indirectly linked to a small ZFS).[45] Moreover, a recent study, which refers to [Gd.TPATCN] as Gd-NO_3Pic, calculated D to be 485 ± 20 MHz (σ_D = 155 ± 37 MHz), much smaller than the DOTA complex (calculated to be 714 ± 43 MHz, σ_D = 328 ± 99 MHz) used most often as the parent compound of spin labels described as having a small ZFS.[20] This publication sets a new standard in extracting the ZFS parameters from EPR data: prior D values have been found using a variety of fitting methods which, while self-consistent, cannot be quantitatively compared. We therefore report the FWHH of our echo-detected field sweep spectra which can be directly compared to the FWHH data reported in the literature, and provide an indication of the magnitude of the ZFS.

Here, we modify [Gd.TPATCN] to produce the compact, water soluble and cysteine-thiol specific spin label [Gd.sTPATCN]-SL to allow bioconjugation. The aim of this work is to demonstrate the rational design of a label in order to maintain a small ZFS by minimizing the effect of breaking the symmetry of [Gd.TPATCN] while providing a thioether linkage. For example, by using a 4-nitropyridine functionality, the new label should have a similar length from the Gd(III) to the protein as MTSSL and bind through a thioether.[46] This can be seen from the deposited crystal structure of [Gd.TPATCN] (CSD-206377) where the distance from the 4-position of the pyridine to Gd(III) is 0.53 nm.[43] This distance is comparable to the distance between the sulfur and the midway point of the nitroxyl radical for the commonly used cysteine-selective nitroxide spin label ((1-oxyl-2,2,5,5-tetramethyl pyrroline-3-methyl)methanethiosulfonate) (MTSSL) which is 0.55 nm in the crystal structure (see Figure S17).[47] Though the conformational flexibilities of the two tethers would be expected to be quite different.

To test the selective conjugation of the label to cysteine, [Gd.sTPATCN]-SL was used to label the synthetic peptide, Ac-GASDYQRLGC-OH and the coiled-coil (cc) domain of the tripartite motif protein family member 25 (TRIM25cc) engineered to contain a single cysteine residue: the natural cysteine residues from TRIM25cc were removed and a single cysteine variant, R236C, was introduced. TRIM25cc has previously been crystalized (PDBID:4LTB), showing the formation of an anti-parallel homodimer.[48] In this crystal the distance between the C_α atoms of R236 of each monomer is 4.25 nm. While we know from previous (unpublished) work that the TRIM25cc in solution does not have the same structure as the crystal, we were confident that this labeling site would position the [Gd.sTPATCN]-SL at a distance greater than 4 nm. This removes ambiguity in the analysis of the DEER data that may be caused by not being able to achieve sufficient bandwidth in our experiments with our commercial Q-band spectrometer for Gd(III) spin labels with small ZFS.[2,23,25,30] The distance was also strategically chosen to test the T_m of the label-protein conjugate to ensure that the DEER time trace could be of sufficient length to measure the dipolar coupling frequency required for the distance. To test the scope of [Gd.sTPATCN]-SL at Q- and W-band frequencies, the DEER measurements were performed on a mixed-labeled TRIM25cc R236C sample which had both [Gd.sTPATCN]-SL and MTSSL attached, to simulate the spectroscopically orthogonal labeling approach. This is similar to the methodology introduced previously, though here the biomolecule is first labeled with the Gd(III) label which we find is kinetically slow, and then with MTSSL rather than mixing pre-labeled protein together.[16]

Scheme 1. Synthesis of required picolinic acid derivatives.

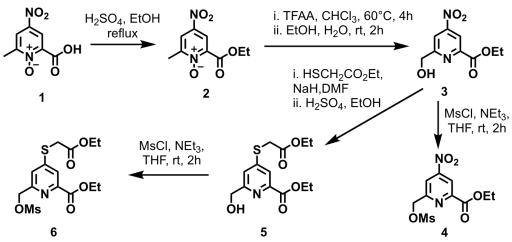

Scheme 2. Synthesis of [Gd.sTPATCN].

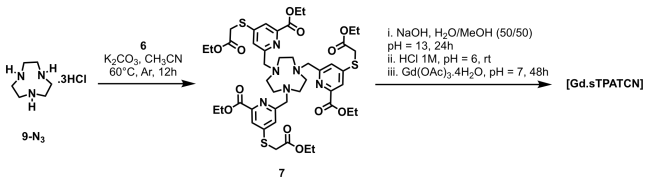

EXPERIMENTAL SECTION

Synthesis and Materials. *Synthesis of [Gd.sTPATCN]-SL.* [Gd.TPATCN] was modified by introducing the 4-((carboxymethyl)thio)picolinic acid moiety to increase the water solubility of the final spin label. As outlined in Scheme 1, the ligand was prepared from 4-nitropicolinic acid **1** in four steps involving esterification of 4-nitropicolinic acid to **2**, an acyl transfer from the trifluoroacetic anhydride (TFAA) to the oxygen of the N-oxide followed by a Boekelheide rearrangement to selectively functionalize the 6-methyl group to afford **3**,[49] reaction with ethyl thioglycolate leading to substitution of the nitro group to give **5**, and mesylation using triethylamine and methanesulfonyl chloride (MsCl) to give a reactive sulfonate ester electrophile **6**. Alkylation of 1,4,7-triazacyclononane (9-N_3) with the mesylate **6** gave the ligand **7**, followed by base hydrolysis and reaction with gadolinium triacetate at pH 7 to yield the C_3-symmetric complex, [Gd.sTPATCN], following pH adjustment and HPLC purification (Scheme 2, 23% overall yield). Importantly, this procedure could be readily modified to produce the asymmetrically substituted complex [Gd.sTPATCN]-SL (Scheme 3, 15% overall yield), made by stepwise alkylation reactions, using the carbamate, BOC-9-N_3 as a precursor and 4-nitropyridine as the site for labeling through conjugation to a cysteine thiol.

Protein production, purification, labeling and preparation of EPR samples. The pET28a-TRIM25cc plasmid vector with a His-SUMO leader sequence (a kind gift from Owen Pornillos),[48] had natural cysteine residues removed and the R236C mutation introduced using QuikChange site directed mutagenesis (Qiagen). Mutations were verified by sequencing (MRCPPU, College of Life Sciences, University of Dundee, Scotland) on a Biosystems model 3730 automated capillary DNA sequencer using Applied Biosystems Big-Dye Version 3.1.

The pET28a-TRIM25cc R236C plasmid was transformed into BL21-DE3 chemically competent cells and plated onto lysogeny broth (LB)-agar plates containing 50 μg/ml kanamycin (kan) using standard procedures. A single colony

Scheme 3. Synthesis of [Gd.sTPATCN]-SL.

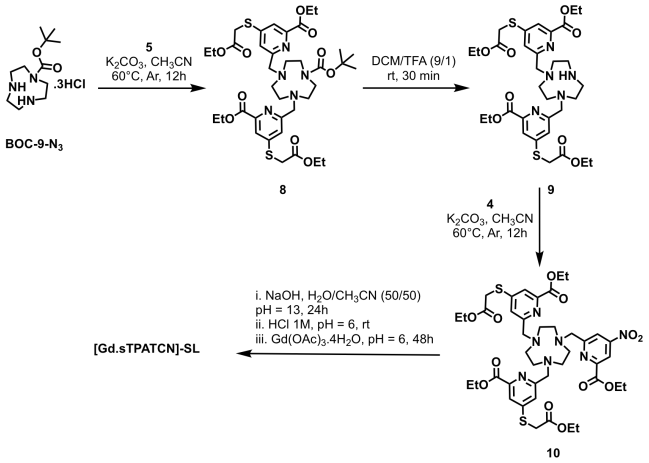

was selected for growth in 10 ml LB containing 50 μg/ml kan overnight at 37°C, 200 rpm. The 10 ml overnight culture was used to inoculate 1 l LB-kan and was grown to an O.D.$_{600}$ of 0.6 at 37°C, 200 rpm, before TRIM25cc R236C expression was induced using 1 mM isopropyl β-D-1-thiogalactopyranoside (IPTG) for 4 h. The cells were pelleted by centrifugation (15900 × g, 0.5 h) and frozen until use. The cell pellets were suspended in 30 ml lysis buffer (30 mM Tris, 300 mM NaCl, pH 9) with 100 μM phenylmethanesulfonyl fluoride (PMSF) protease inhibitor solution in ethanol. The suspended pellets were sonicated using 6 × 30 s pulses (20 μm amplitude) on ice with 30 s breaks between each pulse. The cellular debris was removed by centrifugation (45000 × g, 30 min), and the supernatant was passed through a 5 ml HisTrap™ HP column prepacked with Ni Sepharose (GE Healthcare Life Sciences) pre-equilibrated with lysis buffer. The column was washed through with 2 column volumes (CV) of lysis buffer, then 2 CV wash buffer (25 mM Tris, 100 mM NaCl, 20 mM imidazole, pH 8). The TRIM25cc R236C was eluted in 3 CV elution buffer (25 mM Tris, 100 mM NaCl, 200 mM imidazole, pH 8) and treated with 10 mM DTT for 0.5 h at room temperature.

Size exclusion chromatography (SEC) was used to purify the TRIM25cc R236C further and remove all traces of DTT. The SEC was performed with a HiLoad Superdex 75 pg preparative column with 3 CV SEC buffer (10 mM Tris, 100 mM NaCl, pH 8) and run at 1 ml/min after the TRIM25cc R236C was loaded using a 1 ml sample loop. Protein elution occurred within 50 min in the SEC buffer and the protein containing fractions, determined by the chromatogram (Figure S2), were pooled. The fractions containing the purified TRIM25cc R236C protein was determined by gel electrophoresis (Figure S3). The fractions were pooled after gel electrophoresis to give the pure TRIM25cc R236C protein. This was subsequently concentrated to 200 μl, 100 μM (determined by the absorbance at 280 nm) using a Vivaspin 500 μl centrifugal concentrator column with 10 kDa molecular weight cut off, and labeled with 50 eq. [Gd.sTPATCN]-SL, 16 h, room temperature on a rotating frame. For the labeling carried out in this work the [Gd.sTPATCN]-SL was added to the required concentration from solid stock but since it is easily water soluble a concentrated stock could be prepared if desired. Following centrifugation to remove any precipitate, the excess label was removed using a His SpinTrap 100 μl column (GE Healthcare Life Sciences) by washing with SEC buffer until no [Gd.sTPATCN]-SL was detected in the washes using 280 nm absorbance, equating to 5 CV. Elution buffer was then used to free the protein from the resin.

The mixed-labeled TRIM25cc R236C was prepared by mixing protein with 50 eq. [Gd.sTPATCN]-SL for 11 h rotating at room temperature. The unreacted [Gd.sTPATCN]-SL was removed as above to give 70% [Gd.sTPATCN]-TRIM25cc R236C as confirmed by LC-MS at the University of St Andrews (details below and Figure S6). Subsequently, 5 eq. MTSSL from a concentrated DMSO stock (0.095 M) was added and left at RT for 2 h. The excess MTSSL was removed by washing through the Vivaspin concentrator five times before buffer exchange to D_2O, 20 mM Tris, 200 mM NaCl, pH 8 by washing through the concentrator a further five times. A Bradford assay (using a Bovine Serum Albumin calibration curve) was performed to assess concentration. R1-[Gd.sTPATCN]-TRIM25cc R236C sample was flash frozen in a 3 mm O.D. suprasil EPR tube with 50% glycerol-d_8. The final sample was 60 μl (Q-band) or 80 μl (W-band) with approximately 85 μM R1-[Gd.sTPATCN]-TRIM25cc R236C (mixed label) monomer concentration.

The fully-MTSSL-labeled R1-TRIM25cc R236C sample was prepared by adding 10 eq. MTSSL to purified TRIM25cc R236C at 4°C for 12 h on a rotating frame. The excess label was removed by washing through the Vivaspin concentrator five times before buffer exchange to D_2O, 20 mM Tris, 200 mM NaCl, pH 8 by washing through the concentrator a further five times. A Bradford assay (using a Bovine Serum Albumin calibration curve) was performed to assess concentration. The R1-TRIM25cc sample was flash frozen in a 3 mm O.D. suprasil EPR tube with 50% glycerol-d_8 The final sample was 60 μl with approximately 12 μM R1-TRIM25cc R236C monomer concentration. EPR samples were visually inspected before and after freezing for any signs of precipitation, and were found to be clear.

Details of the labeling the synthetic peptide Ac-GASDYQRLGC-OH can be found in the Supporting Information.

The samples for the pulsed EPR measurements of the Gd(III) complexes were prepared by dissolving the lyophilized complexes in H_2O/glycerol (1:1 v/v) or D_2O/glycerol-d_8 (1:1 v/v) to give 20 μM solutions. They were measured as frozen solutions in 3 mm O.D. suprasil EPR tubes.

Mass spectrometry. LC-MS and LC ESI MSMS was performed on a QToF Premier equipped with an Acquity UPLC (Waters Corp) to confirm both the synthesis of the Gd(III) complexes and the modification of the synthetic peptide [Gd.sTPATCN]-Ac-GASDYQRLGC-OH. Reverse phase gradient separation was achieved using an Acquity UPLC BEH C18 column 1.7 μm (2.1 mm × 100 mm) (Waters Corp.). The 0.4 ml/min solvent gradient ran from 100% water containing 0.1% formic acid to 100% acetonitrile over 5 min.

Positive ions from the electrospray ion source were recorded as a full MS spectrum. The desired precursor ion was mass selected by the quadrupole with an isolation window that transmitted the full isotopic envelope. Collision induced dissociation was performed in the quadrupole with argon as the collision gas. Here, the collision energy was ramped from 25 eV to 45 eV and the resulting MSMS spectrum recorded.

A reference spray provided a "lock mass" that enable a cal-

ibration correction for accurate mass determination of both the MS and MSMS data.

The intact protein analysis was performed on a QToF Premier equipped with an Acquity UPLC (Waters Corp.). The protein sample was desalted on-line using a Waters MassPREP on-line desalting cartridge. The 0.4 ml/min solvent gradient ran from 95% water (containing 0.1% formic acid):5% acetonitrile to 20% water (containing 0.1% formic acid):80% acetonitrile over 5 min. Positive ions from the electrospray ion source were recorded over the mas range 800-2000 u. Protein data are processed using Masslynx 4.1 and deconvoluted using MaxEnt 1 to show the nominal neutral mass of the protein

The peptides resulting from the tryptic digest were analysed on a Synapt G2s HDMS equipped with an Acquity i-class UPLC (Waters Corp.). Reverse phase gradient separation was achieved using an Acquity UPLC BEH C18 column 1.7 μm (2.1 mm $\times$ 100 mm) (Waters Corp.). The 0.2 ml/min solvent gradient ran from 99% water containing 0.1% formic acid to 50% acetonitrile containing 0.1% formic acid over 40 min before re-equilibration. 3 μl was injected for the MS analysis; 5 μl injected for the MSMS.

Positive ions from the electrospray ion source were recorded as a full mass spectrum. For MSMS, the desired precursor ion was mass selected by the quadrupole with an isolation window that transmitted the full isotopic envelope. Collision induced dissociation was performed in the trap region of the Triwave. Here, the collision energy was ramped from 20 eV to 30 eV and the resulting MSMS spectrum recorded.

A reference spray provided a "lock mass" that enable a calibration correction for accurate mass determination of both the MS and MSMS data.

LC-MS at the University of St Andrews was analysed on a Waters 2795 HPLC and LCT, desalting with a Waters MassPrep on-line desalting column, eluting with an increasing gradient of acetonitrile. The masses were calibrated against horse heart myoglobin and the charge envelope was deconvoluted using MaxEnt1.

EPR experiments. Pulsed EPR measurements were carried out either with the high-power (150 W) Q-band (34 GHz) Bruker Elexsys E580 with an ER 5106QT-2w cylindrical resonator or the home-built high power (1 kW) W-band (94 GHz) "HiPER" spectrometer.[34,35]

Echo-detected field sweeps. The echo-detected field sweeps were taken using a Hahn echo $\frac{\pi}{2} - \tau - \pi - \tau - echo$ pulse sequence. For Q-band the $\frac{\pi}{2}$ and π pulse durations were 16 and 32 ns respectively, the interpulse delay, τ was 200 ns and the shot repetition time (SRT) was 2 ms. The measurement temperature was 10 K. At W-band the measurements were carried out at 9.8 K using $\frac{\pi}{2}$ and π pulse durations of 4 ns and 8 ns respectively, τ of 300 ns, a sequence repetition frequency of 3 kHz and 3000 shots per point. The FWHH was measured by normalizing the spectrum to its maximum and measuring its width at the half intensity point using the plot function in Matlab.

Relaxation measurements. Relaxation data were collected at Q-band. T_1 was measured using an inversion recovery sequence $\pi - t - \frac{\pi}{2} - \tau - \pi - \tau - echo$ at the field corresponding to the maximum of the absorption spectrum. These measurements were also performed at 10, 20 and 50 K for all of the Gd(III) complexes, as well as at 7 K for [Gd.sTPATCN]-SL and [Gd.sTPATCN]-peptide with a $\frac{\pi}{2}$ of 16 ns and π pulse of 32 ns and t and τ values varying depending upon requirement (Figure S10). The data were fit using the Xepr software with a bi-exponential curve. The T_1 values are presented in Table S3 assuming a Bloch model for relaxation and are found at intensity value of 0.26 using Matlab, where the fully recovered magnetization has an intensity of one.

T_m was measured at the maximum intensity of the echo-detected field sweep spectrum using a $\frac{\pi}{2} - \tau - \pi - \tau - echo$ pulse sequence to see the echo decay with increasing interpulse delay. The $\frac{\pi}{2}$ was 16 ns, the π pulse 32 ns, acquiring 32 ns around the top of the echo with an initial τ of 200 ns for all of the Gd(III) complexes and 220 ns for the R1-[Gd.sTPATCN]-TRIM25cc R236C sample. This was incremented in 8 ns steps. Measurements were taken at 10, 20 and 50 K for all of the Gd(III) complexes, as well as at 7 K for [Gd.sTPATCN]-SL and [Gd.sTPATCN]-peptide. The SRT was dependent upon temperature, with 2 ms at 50 K, 5 ms at 20 and 10 K. A two-step phase cycle was also applied. The resultant echo decay curves (Figure S9) were fitted with a stretched exponential decay using the Xepr software and parameters are reported in Table S2. The T_m values presented in Table 1 are 10% values of T_m found using the Matlab plot function rather than the stretched exponential decay fit values, as this is what is commonly reported in the literature. There is a small variation in the T_m measurement each time a sample is re-measured and we estimate an error of about 0.1 μs for the data in Table 1. T_1 and T_m measurements were also taken at various field positions (Figures S11-13).

DEER. DEER experiments were carried out using a four-pulse, deadtime free sequence $(\frac{\pi}{2}(observe) - \tau_1 - \pi(observe) - t - \pi(pump) - (\tau_1 + \tau_2 - t) - \pi(observe) - \tau_2 - echo)$ on R1-[Gd-sTPATCN]-TRIM25cc R236C.[18,19] For the Q-band measurements, the cavity was over-coupled following standard procedure such that the matched minimum occurs at 34.0 GHz. The variable experimental parameters, including the frequency of the pump and observer pulses, are in Table S4. The pump pulse was set on the top of the Gd(III) absorption spectrum for experiments 2 and 4 and on the maximum of the nitroxide absorption spectrum for experiments 3 and 5. The observer sequence used 32 ns $\frac{\pi}{2}$ and π pulses and t was stepped in 8 ns increments. The SRT was optimized to measure at least 70% of the echo height and for each scan, 30 shots were taken at each time point except for experiment 2, which used 16 shots per point. A two-step phase cycle with nuclear modulation averaging (5 steps of 24 ns separation with an initial τ_1 of 400 ns) was applied.

The W-band DEER experiments were performed at 9.8 K. The pump pulse was set at the top of the Gd(III) absorption spectrum, and an 8 ns pump pulse was used. The $\frac{\pi}{2}$ was 4 ns, the π pulse 8 ns for the observer sequence. The inter-pulse τ_1 and τ_2 were set at 300 ns and 8400 ns respectively and the pump pulse was incremented in 40 ns steps with 201 data points. The observer pulse sequence was set at an offset of 420 MHz. As with the field sweep, the sequence repetition frequency used was 3 kHz, averaging 3000 shots per point.

DeerAnalysis2018 was used to process the DEER data.[26] Artefacts were removed by cutting 800 ns from the end of all the time traces taken at Q-band. The zerotime was set at 329 ns except experiment 4 (322 ns) and 1 (141 ns), and a three-dimensional homogeneous background was assumed. The "noisy" option, implemented in DeerAnalysis2018, was used to avoid artefacts at the very beginning of the data set (before the zerotime) effecting the modulation depth results. The Tikhonov Regularization parameter was generated as the best choice by DeerAnalysis2018, given in Table S4.

The data and results for a τ_2 of 6 μs Gd(III)-Gd(III) experiment at Q-band (experiment 6) are presented in Figure S14.

RESULTS AND DISCUSSION

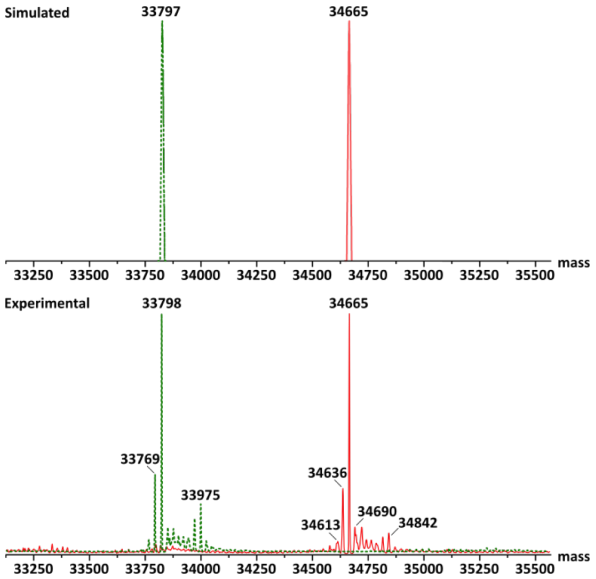

Figure 2. ESI QTOF MS results confirming the selective conjugation of [Gd.sTPATCN]-SL with TRIM25cc R236C to give [Gd.sTPATCN]-TRIM25cc R236C. The green mass spectra indicate simulated (top) and experimental (bottom) masses for TRIM25cc R236C. The red spectra indicate simulated (top) and experimental (bottom) masses for [Gd.sTPATCN]-TRIM25cc R236C. The red experimental spectrum shows no peak corresponding to the mass of unlabeled protein, demonstrating $>$ 95% labeling in the [Gd.sTPATCN]-TRIM25cc R236C. The simulated masses correspond well to the experimental results.

[Gd.TPATCN], [Gd.sTPATCN] and [Gd.sTPATCN]-SL were synthesized. The [Gd.sTPATCN]-SL was used to label the synthetic peptide Ac-GASDYQRLGC-OH (ammonium bicarbonate buffer at pH 7.8, 1 eq label, RT, 72 h) and TRIM25cc R236C (Tris NaCl buffer at pH 8.0, 50 eq label, RT, 16 h) at cysteine. The labeling of the peptide was monitored by LC-MS and selective modification of the cysteine was verified by MS/MS fragment analysis (Figure S1). Electrospray ionization (QToF-MS) of the TRIM25cc R236C indicated $>$ 95% labeling, giving m/e = 33797.6 (calc. for [M-Met] 33797.4) for the native protein and 34665 (calc. 34665) for the [Gd.sTPATCN]-labeled conjugate wherein the N-terminal methionine cleaves under the analysis conditions and the cysteine residue is bound to the Gd(III) complex with displacement of the 4-nitro group (Figure 2). LC-ESI MS/MS analysis of a trypsin digest of the conjugated protein gave unequivocal evidence for selective linkage of [Gd.sTPATCN]-SL to the cysteine residue, consistent with the site-specific labeling hypothesis (Figure S5).

The conditions for labeling the protein are similar, though the reaction time is longer ($>$ 95% yield, 16 h, RT), to those reported for [Gd.DO3MA-3BrPy]. This label was reported to label with an 80% yield in six hours at room temperature.[9] We utilized the slow labeling rate to allow production of a mixed-labeled TRIM25cc R236C with [Gd.sTPATCN]-SL and the nitroxide label MTSSL, to test the Gd(III) label for DEER and to simultaneously demonstrate its scope as a spectroscopically-orthogonal label to nitroxides. The protein was intentionality under-labeled with [Gd.sTPATCN]-SL, by leaving it to react for only 11 h at room temperature to attain 70% labeling (as opposed to 16 h for full labeling) as assessed by LC-MS (see Figure S6). The remaining free cysteines were then reacted with MTSSL to give R1-[Gd.sTPATCN]-TRIM25cc R236C where R1 is the nitroxide spin label. For comparative purposes, an R1-TRIM25cc R236C sample was also prepared. The modulation depth of the DEER data for R1-TRIM25cc R236C was close to 30% which is the typical value we measure in this set-up for full MTSSL labeling. Given the measured good reactivity of MTSSL with the TRIM25cc R236C cysteines, we inferred that all cysteines remaining after 11 h incubation with [Gd.sTPATCN]-SL had reacted with MTSSL. Therefore, we expected R1-[Gd.sTPATCN]-TRIM25cc R236C to be labeled with 70% Gd(III) and 30% nitroxide and, assuming non-cooperative labeling, the protein in solution comprises of approximately 49% double-[Gd.sTPATCN]-SL-labeled dimers (21 μM dimer), 42% mixed Gd(III)-nitroxide dimers (18 μM dimer) and 9% double-nitroxide-labeled dimers (4 μM dimer).

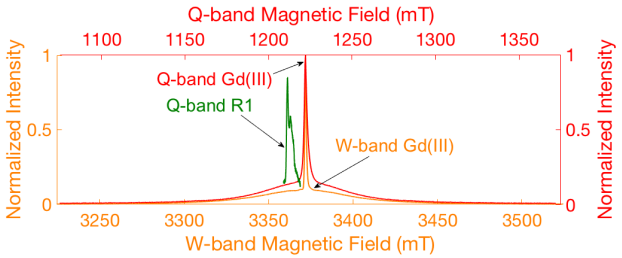

Figure 3. The Q-band echo-detected field sweeps of R1-[Gd.sTPATCN]-TRIM25cc R236C: nitroxide and Gd(III) at Q-band, 10 K (green and red respectively) and Gd(III) at W-band, 9.8 K (orange).

The echo-detected field swept spectra (34 GHz, 10 K) for the compounds in water/glycerol solution are characteristic of Gd(III) complexes with a small ZFS. The FWHH of the absorption spectrum, corresponding to the central transition of all the studied samples, are presented in Table 1. The FWHH of symmetrically modified [Gd.sTPATCN] is larger than the parent compound and increases further for the asymmetric nitro complex [Gd.sTPATCN]-SL, from 1.72 mT to 2.10 mT to 3.58 mT in the same solvent mixture. These changes are to be expected: the ligand field created by the TPATCN ligand containing either Eu(III), Dy(III) or Yb(III) is very sensitive to small changes in its local environment, and these changes would be expected to impact on the ZFS for Gd(III).[50]

Encouragingly, conjugation to the peptide Ac-GASDYQRLGC-OH or protein TRIM25cc R236C decreases the observed FWHH (Table 1). This is consistent with our hypothesis that the complex should have a higher symmetry, and therefore smaller ZFS, when bound to a thiol. For the mixed-labeled R1-[Gd.sTPATCN]-TRIM25cc R236C the FWHH of the echo-detected field swept spectrum is 2.54 mT at Q-band (34 GHz, 10 K) and 1.14 mT at W-band (94 GHz, 9.8 K), see Figure 3. This W-band measurement is comparable to the narrowest central transition for a Gd(III) spin label attached to a protein reported to date.[27,30,40]

We present the time taken for the echo to decay by 90% to indicate the T_m to aid comparison to the literature and also because this is a useful practical number for the ability to measure the DEER time trace out to longer times. Longer time DEER measurements allow the capture of lower frequency dipole-dipole coupling and therefore longer inter-

Table 1. FWHH for the central line of the echo-detected field sweep, and the time for echo to decay to 10% original value as an indicator of T_m from Q-band pulsed EPR for the Gd(III) complexes synthesized here. The solutions were 20 μM in H_2O 50% glycerol at 34 GHz, 10 K except [a]D_2O, 50% glycerol-d_8 and [b]buffer in D_2O, 50% glycerol-d_8.

Sample	FWHH (mT)	10% signal (μs)
[Gd.TPATCN]	1.72	6.5
[Gd.sTPATCN]	2.10	6.5
[Gd.sTPATCN]-SL	3.58	6.5
[Gd.sTPATCN]-SL[a]	3.36	52.6
[Gd.sTPATCN]-Ac-GASDYQRLGC-OH	2.03	6.6
R1-[Gd.sTPATCN]-TRIM25cc R236C[b]	2.54	12.6

spin distances. The decay times do not vary with the FWHH of the spectrum but are dependent upon deuteration, as has been observed previously.[4,7,51–53] Thus we measure the protein in a deuterium-containing solvent mixture as a convenient method to increase the T_m, but deuteration of the protein would certainly lead to further improvements.[53]

The 10% value for R1-[Gd.sTPATCN]-TRIM25cc R236C (Q-band, 10 K) is 12.6 μs (Figure 4a), which is longer than Gd(III) spin labels on proteins in similar solvent mixtures: the values are reported in the supplementary material of the corresponding literature as approximately 6 μs for [Gd.C1] (and [Gd.C9])[41] and 5 μs for [Gd.DO3MA-3BrPy][9] at W-band, 10 K. The recent study that removes the methyl groups from [Gd.DO3MA-3BrPy] reports an extension of the T_m time and inspection of the two-pulse echo decay curve in the paper gives an approximate 10% value of just less than 9 μs. Although the value of T_m will depend upon the protein variant, the improvement in T_m for [Gd.sTPATCN]-SL appears significant. The [Gd.TPATCN]-based complexes still have a reasonable T_m in H_2O/glycerol (Table S2) which makes the label a promising candidate for increased measurement sensitivity for in-cell applications, where deuteration of the cellular environment may not be possible.

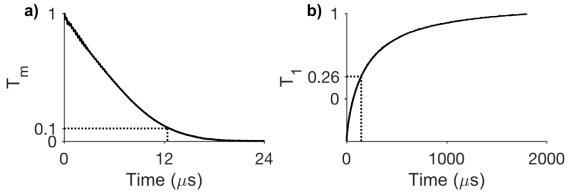

Figure 4. a) The echo-decay and b) inversion recovery curves for R1-[Gd.sTPATCN]-TRIM25cc R236C (buffer in D_2O, 50% glycerol-d_8, 10 K, Q-band). The 10% value is labeled with dashed lines for the T_m and 0.26 intensity for T_1 is also labeled. These relaxation measurements were collected during the same measurement period as the DEER experiments.

We also measured the echo-decay curves at various field positions of the R1-[Gd.sTPATCN]-TRIM25cc R236C Gd(III) spectrum to probe the T_m of different transitions (see Figures S11-S13). In agreement with the literature, we found that the longest decay curve corresponds to the central transition.[51] At a field separation from the maximum of the Gd(III) lineshape of 12 mT (335 MHz, Q-band), only a minor decline of the T_m and corresponding 10% value is observed (13% decrease in 10% echo decay value). This therefore does not deter from setting the DEER observer pulse sequence here: we set our pump pulse on the maximum of the Gd(III) signal to optimize the modulation depth in the DEER and our observer pulses offset from the central transition.

Figure 4b presents the Gd(III) inversion recovery curve as a measure of T_1 for R1-[Gd.sTPATCN]-TRIM25cc R236C at 10 K which is fast at around 230 μs for the maximum of the central transition. Moving off the central transition slightly reduces the T_1 (Figure S12). The short T_1 allows for fast signal averaging at 10 K.

Inter-Gd(III) DEER experimental measurements with R1-[Gd.sTPATCN]-TRIM25cc R236C were made at Q- and W-band (Figure 5b, data sets 2 and 1 respectively). The T_m at 10 K allowed for a DEER measurement window of 9 μs, which would be sufficient for distance measurements up to c.a. 8 nm.[55] The dipolar frequency measured was insensitive to the frequency of the experiment which indicated that this coupling range could be measured well at both frequencies without a significant component from the pseudo-secular dipolar terms.

The pump pulse was set on the maximum of the Gd(III). At Q-band both the pump and observer pulses were offset from the minimum of the over-coupled cavity to maximize their frequency difference while maintaining a reasonable level of available power.[56] Therefore 14 ns was the shortest pump pulse we could use while retaining 32 ns observer pulse lengths. We also found that 14 ns was an optimal length for inverting the echo at the maximum of the Gd(III) spectrum, even at the matched frequency of the cavity (34.0 GHz) where there is sufficient power for shorter pulses. This was unexpected since while an $S = \frac{1}{2}$ center, such as a nitroxide, typically has DEER acquired with a 14 ns pump pulse with the power available in our spectrometer, the higher transition probability of the $S = \frac{7}{2}$ Gd(III) should enable a shorter pulse length. In fact, in unpublished work for other, less narrow spectrum Gd(III) complexes we were able to use a 4 ns π pump-pulse. We did not encounter this behavior during the W-band optimization and used a pump pulse length of 8 ns.

Although the two measurements are not directly comparable, due to differences in their set-up including the length of the DEER time trace, we observed that at W-band there was a significant increase in sensitivity compared to Q-band and were able to obtain the data in approximately 2.5 hours rather than overnight (SRT, shots per point and number of averages are presented in Table S4 of the Supporting Information). The close agreement between Q- and W-band Gd(III)-Gd(III) data, which have very similar modulation depths and dipole-dipole coupling measurements, demonstrates that [Gd.sTPATCN]-SL is useful in this dipolar coupling regime at Q-band on a commercial spectrometer.

The R1-[Gd.sTPATCN]-TRIM25cc R236C experimentally-measured modulation depth of the Q- and W-band Gd(III)-Gd(III) DEER data presented in Figure 5b is 9%. During the DEER set-up we noticed some variation with the frequency separation between the observer and pump pulses (see Figure S16) but we did not systematically optimize our experiments for modulation depth by varying the frequency separation or temperature, and so 9% may not have been the absolute maximum for our sample. We cannot readily explain the coincidence in the modulation depth at the two frequencies, but the observation of a 9% modulation depth is particularly gratifying considering that this is a 70% Gd(III)-labeled monomer, equivalent to only approximately half the dimers being doubly labeled with [Gd-sTPATCN]-SL. The dimers that are Gd(III) and nitroxide labeled (around 42%) will contribute to the background decay function and therefore a decrease in modulation depth.[12,16] Our λ is at the upper end of the published modulation depths for Gd(III)-Gd(III) DEER data at both

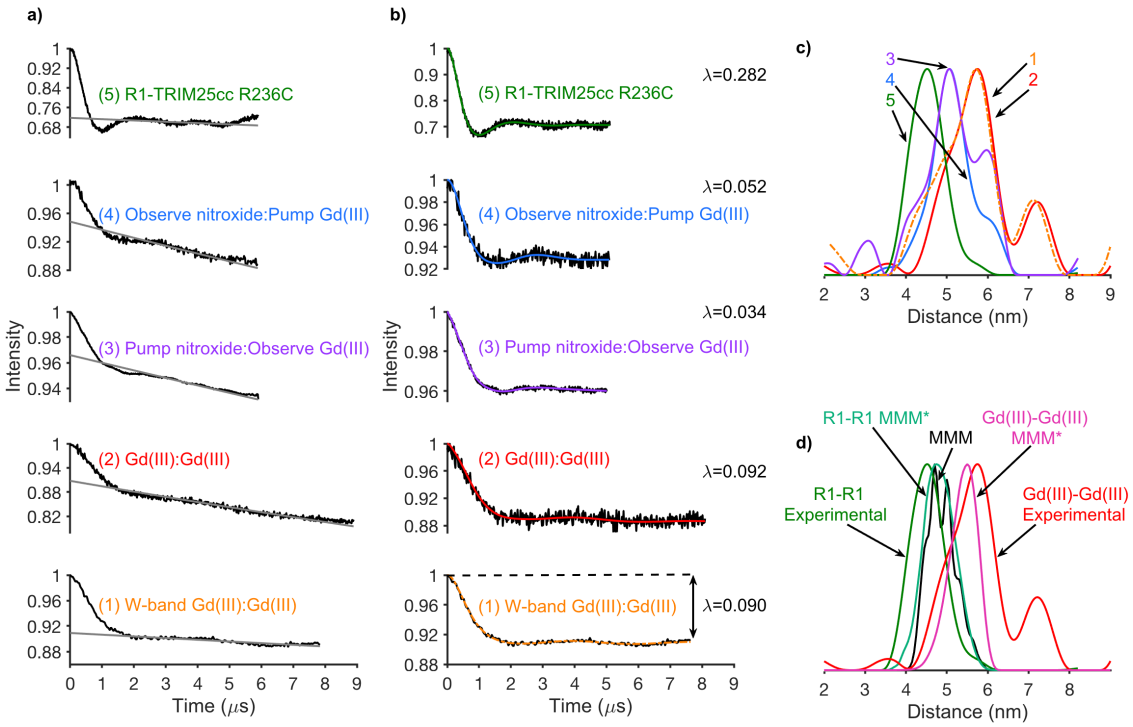

Figure 5. DEER data for TRIM25cc R236C, either fully labeled with R1 (R1-TRIM25cc R236C), or labeled with both R1 and [Gd.sTPATCN] (R1-[Gd.sTPATCN]-TRIM25cc R236C). a) DEER time traces: (1) and (2) Gd(III)-Gd(III) at 10 K W- and Q-band respectively; (3) and (4) nitroxide-Gd(III) at 10 K, Q-band and (5) nitroxide-nitroxide in R1-TRIM25cc R236C (50 K, Q-band). The fitted background correction is shown as a grey line. b) Background corrected DEER time traces with the corresponding fits from Tikhonov Regularization with DeerAnalysis2018 (further details in the Supporting Information).[26] The modulation depths, λ, are also presented. c) The distance distributions for the DEER time traces in (a) and (b) calculated with Tikhonov Regularization. d) Experimental and modeled distance distributions of TRIM25cc R236C. The black distance distribution was calculated using MMM 2018.1 by modeling MTSSL rotamers onto the R236 position on each monomer of the TRIM25cc crystal structure (PDBID:4LTB).[48,54] The fits denoted by MMM* (turquoise and magenta) were also produced by MMM 2018.1 through selecting rotamers to fit the individual experimental data (green and red).

frequencies.[2,41,57] We attempted to measure a fully-labeled [Gd.sTPATCN]-TRIM25cc R236C sample but we found that, in this case, there appeared to be a significant amount of free [Gd.sTPATCN]-SL around which disrupted the experiments. The evidence for the free label and the DEER results are shown in Figures S18 and S19. The non-specific binding of Gd(III) label has been observed previously by others, and its removal will need to be further investigated during future development of the labeling protocol.[12]

Previous studies have theoretically estimated the modulation depth of Gd(III)-Gd(III) DEER through assuming that the pump pulse is set to the maximum of the central transition but does not have sufficient bandwidth to invert it all (15 ns for a ZFS D parameter of 1000 MHz). These have found that the theoretical maximum λ is around 20% at 25 K.[2] Similar upper limits were calculated in a more recent work with a range of ZFS values.[25] This theoretical maximum has not been measured using the standard four-pulse DEER experiment, though utilizing two chirped pump pulses in a modified Q-band DEER experiment have enabled larger modulation depths up to 20%.[2,17,31,32,57] We conclude that the reduction in measured modulation depth for [Gd.sTPATCN]-SL compared to theoretical estimates is less than for other existing Gd(III) spin labels.

The nitroxide-Gd(III) dipolar coupling was measured using two protocols at Q-band. The first protocol set the pump pulse frequency to the maximum of the nitroxide absorption and the observer pulse to the maximum of the Gd(III) signal (Figure 5b, data set 3), the second protocol reversed the frequencies (Figure 5b, data set 4). Setting the observer frequency on the Gd(III), as in data set 3, allows a 400 times faster repetition rate than for data set 4 due to differences in the T_1 values for Gd(III) and nitroxide at 10 K. Thus, this experiment is optimal for signal accumulation. If there were no spectral overlap between the nitroxide and the Gd(III), this protocol should give the better modulation depth too since a shorter pump pulse is attainable in our Q-band spectrometer due to cavity bandwidth limitations (14 ns on the nitroxide in experiment 3 rather than 28 ns on the Gd(III) in experiment 4) and also a greater proportion of the nitroxide spins can be pumped due to its narrower spectrum.[3,16] In practice, setting the pump pulse on the nitroxide causes echo and modulation depth reduction due to Gd(III) transitions also being excited.[14,16,17] The combined effect is a slightly greater modulation depth for experiment 4 than experiment 3.

The difference in spectroscopic properties between Gd(III) and nitroxides allow specificity in the measurement between Gd(III)-Gd(III) distances and Gd(III)-nitroxide distances despite the spectral overlap.[11,17] A study that used two Gd(III) labels and one nitroxide label, was analyzed in terms of the different pulse power levels required for Gd(III) (observed) and nitroxide (pumped), and concluded that the different contributions could not be fully separated.[14] We

notice that the distribution of distances for experiment 4 is smaller than the distribution measured by experiment 3 (Figure 5c). This is consistent with the experiment measuring both Gd(III)- Gd(III) and Gd(III)-nitroxide distances when the pump pulse frequency is set on the maximum of the nitroxide, but predominantly Gd(III)-nitroxide distances when set on the maximum of the Gd(III). The apparent ability to separate distances arising from Gd(III)-Gd(III) from the Gd(III)-nitroxide interactions through exchanging the pump and observer pulse frequencies and/or moderating their length, has potential for future applications of DEER using spectroscopically orthogonal labels.

The dipole-dipole coupling measured by DEER can be used to determine distances and distributions. The results are displayed in Figure 5c. Unfortunately these distributions are broader than desirable for a model system, which may be a consequence of the conformational freedom of the label or the flexibility of the protein backbone.

The Gd(III)-Gd(III) results at both Q- and W-band have a most probable distance of 5.75 nm with similar standard deviations on their distributions of 0.89 nm and 0.92 nm at Q- and W-band respectively (DeerAnalysis Validations of these distributions are given in Figure S15). The purely nitroxide-labeled R1-TRIM25cc R236C DEER (Figure 5b, data set 5) has a modal distance of 4.51 nm with a standard deviation of 0.43 nm. The Gd(III)-nitroxide from experiment 3 has a most probable distance of 5.17 nm (standard deviation 0.52 nm). Comparing the distance results from these three DEER experiments indicates that the [Gd.sTPATCN] moiety bound to the protein occupies a different space to the R1 rotamers despite the very similar tether length for [Gd.sTPATCN]-SL and MTSSL (Figure S17).[43,47]

The broader distribution for Gd(III) spin labels compared to the R1 side chain has been observed previously and attributed to the complexes not interacting strongly with the surrounding protein structure.[2] The observed difference in the distribution width, and the systematic increase in the modal distance measured from nitroxide-nitroxide through to Gd(III)-Gd(III), could be due to both variations in the space occupied by the different labels, and an unfortunate choice of labeling position, where the disparity is most emphasized. We cannot completely discount the possibility that by labeling with the Gd(III) complex, we have caused higher order oligomers to form, which has altered the measured distances and would change the expectation value of the modulation depth.

The solution-state structure of the TRIM25cc is not known and therefore modeling our label onto the existing crystal structures using, for example, the rotamer approach as applied previously by others, may not be helpful.[13] To aid the understanding of our DEER data we used the rotamer approach in the MMM 2018.1 software to model the R1 side chain onto the crystal structure PDBID:4LTB.[48,54] R1 was also used as a surrogate for the [Gd.sTPATCN]-SL since the distance from the atom linked to the cysteine sulfur and the paramagnetic center are about the same (see Figure S17), though the conformations will be different. The results in Figure 5d show that the R1 rotamers do not fit either the R1-R1 distance or the Gd(III)-Gd(III) distance distribution well. With a different population of rotamers, the MMM predictions more closely resemble the experimental data, though still not exactly. These results imply that we do not know the solution-state structure of TRIM25cc, but that the difference in distances we measure are feasible for spin labels of the length we have here.

Having introduced the rational design, synthesis, protein conjugation and preliminary DEER experiments for [Gd.sTPATCN]-SL we next plan to understand the conformations of the label, optimize its use in DEER and compare to other Gd(III) spin labels.

CONCLUSIONS

In summary, we have presented a Gd(III) spin label, [Gd.sTPATCN]-SL, based on the nine-coordinate 9-N_3 tris(pyridine-2-carboxylate) ligand. It is water soluble and conjugates to cysteine residues within proteins with a short thioether tether. The spectroscopic properties of this label give increased sensitivity for distance measurements by DEER through longer echo-decay times than other reported Gd(III) labels, and a narrow central transition linewidth producing a large modulation depth. Overall, [Gd.sTPATCN]-SL is a promising label for expanding the scope and applicability of DEER measurements.

Acknowledgement The authors thank the ERC (266804), EPSRC (EP/R013705/1, EP/M508214/1), and the Carnegie Trust (RIG007510) for financial support, the Wellcome Trust for a Multi-User Equipment Grant (099149/Z/12/Z), and the Royal Society for a University Research Fellowship to JEL. We also thank Professor Catherine Botting and Dr Sally Shirran for assistance with MALDI TOF in St Andrews.

Supporting Information Available: Synthetic methods, spin labeling, sample preparation, mass spectrometric analysis, NMR data and additional EPR data. EPR data underpinning this work is available at DOI: 10.17630/7c07c45b-af1c-4051-a291-65a243b06efc. This material is available free of charge via the Internet at `http://pubs.acs.org/`.

References

(1) Jeschke, G. DEER Distance Measurements on Proteins. *Annu. Rev. Phys. Chem.* **2012**, *63*, 419–446.
(2) Goldfarb, D. Gd(III) Spin Labeling for Distance Measurements by Pulse EPR Spectroscopy. *Phys. Chem. Chem. Phys.* **2014**, *16*, 9685–9699.
(3) Yulikov, M. *Electron Paramagnetic Resonance: Volume 24*; The Royal Society of Chemistry, 2015; Vol. 24; pp 1–31.
(4) Feintuch, A.; Otting, G.; Goldfarb, D. In *Electron Paramagnetic Resonance Investigations of Biological Systems by Using Spin Labels, Spin Probes, and Intrinsic Metal Ions, Part A*; Qin, P. Z., Warncke, K., Eds.; Methods in Enzymology; Academic Press, 2015; Vol. 563; pp 415 – 457.
(5) Haugland, M. M.; Anderson, E. A.; Lovett, J. E. In *Electron Paramagnetic Resonance*; Chechik, V., Murphy, D., Eds.; The Royal Society of Chemistry, 2017; Vol. 25; pp 1–34.
(6) Martorana, A.; Bellapadrona, G.; Feintuch, A.; Di Gregorio, E.; Aime, S.; Goldfarb, D. Probing Protein Conformation in Cells by EPR Distance Measurements using Gd(III) Spin Labeling. *J. Am. Chem. Soc.* **2014**, *136*, 13458–13465.
(7) Qi, M.; Gross, A.; Jeschke, G.; Godt, A.; Drescher, M. [Gd.PyMTA] Label Is Suitable for In-Cell EPR. *J. Am. Chem. Soc.* **2014**, *136*, 15366–15378.
(8) Mascali, F. C.; Ching, H. Y. V.; Rasia, R. M.; Un, S.; Tabares, L. C. Using Genetically Encodable Self-Assembling Gd(III) Spin Labels To Make In-Cell Nanometric Distance Measurements. *Angew. Chem. Int. Ed.* **2016**, *55*, 11041–11043.
(9) Yang, Y.; Yang, F.; Gong, Y. J.; Chen, J. L.; Goldfarb, D.; Su, X. C. A Reactive, Rigid Gd(III) Labeling Tag for In-Cell EPR Distance Measurements in Proteins. *Angew. Chem. Int. Ed.* **2017**, *56*, 2914–2918.
(10) Lueders, P.; Jeschke, G.; Yulikov, M. Double Electron-Electron Resonance Measured Between Gd(III) Ions and Nitroxide Radicals. *J. Phys. Chem. Lett.* **2011**, *2*, 604–609.
(11) Lueders, P.; Jäger, H.; Hemminga, M. A.; Jeschke, G.; Yulikov, M. Distance Measurements on Orthogonally Spin-Labeled Membrane Spanning WALP23 Polypeptides. *J. Phys. Chem. B.* **2013**, *117*, 2061–2068.
(12) Garbuio, L.; Bordignon, E.; Brooks, E. K.; Hubbell, W. L.;

Jeschke, G.; Yulikov, M. Orthogonal Spin Labeling and Gd(III)-Nitroxide Distance Measurements on Bacteriophage T4-Lysozyme. *J. Phys. Chem. B.* **2013**, *117*, 3145–3153.
(13) Gmeiner, C.; Klose, D.; Mileo, E.; Belle, V.; Marque, S. R. A.; Dorn, G.; Allain, F. H. T.; Guigliarelli, B.; Jeschke, G.; Yulikov, M. Orthogonal Tyrosine and Cysteine Site-Directed Spin Labeling for Dipolar Pulse EPR Spectroscopy on Proteins. *J. Phys. Chem. Lett.* **2017**, *8*, 4852–4857.
(14) Gmeiner, C.; Dorn, G.; Allain, F. H. T.; Jeschke, G.; Yulikov, M. Spin Labelling for Integrative Structure Modelling: A Case Study of the Polypyrimidine-Tract Binding Protein 1 Domains in Complexes With Short RNAs. *Phys. Chem. Chem. Phys.* **2017**, *19*, 28360–28380.
(15) Wu, Z.; Feintuch, A.; Collauto, A.; Adams, L. A.; Aurelio, L.; Graham, B.; Otting, G.; Goldfarb, D. Selective Distance Measurements Using Triple Spin Labeling with Gd(III), Mn(II), and a Nitroxide. *J. Phys. Chem. Lett.* **2017**, *8*, 5277–5282.
(16) Kaminker, I.; Yagi, H.; Huber, T.; Feintuch, A.; Otting, G.; Goldfarb, D. Spectroscopic Selection of Distance Measurements in a Protein Dimer With Mixed Nitroxide and Gd(III) Spin Labels. *Phys. Chem. Chem. Phys.* **2012**, *14*, 4355–4358.
(17) Yulikov, M.; Lueders, P.; Warsi, M. F.; Chechik, V.; Jeschke, G. Distance measurements in Au nanoparticles functionalized with nitroxide radicals and [Gd.DTPA] chelate complexes. *Phys. Chem. Chem. Phys.* **2012**, *14*, 10732–10746.
(18) Milov, A.; Ponomarev, A.; Tsvetkov, Y. Electron-Electron Double Resonance in Electron Spin Echo: Model Biradical Systems and the Sensitized Photolysis of Decalin. *Chem. Phys. Lett.* **1984**, *110*, 67–72.
(19) Martin, R. E.; Pannier, M.; Diederich, F.; Gramlich, V.; Hubrich, M.; Spiess, H. W. Determination of End-to-End Distances in a Series of TEMPO Diradicals of up to 2.8 nm Length with a New Four-Pulse Double Electron Electron Resonance Experiment. *Angew. Chem. Int. Ed.* **1998**, *37*, 2833–2837.
(20) Clayton, J. A.; Keller, K.; Qi, M.; Wegner, J.; Koch, V.; Hintz, H.; Godt, A.; Han, S.; Jeschke, G.; Sherwin, M. S.; Yulikov, M. Quantitative Analysis of Zero-Field Splitting Parameter Distributions in Gd(III) Complexes. *Phys. Chem. Chem. Phys.* **2018**, *20*, 10470–10492.
(21) Clayton, J. A.; Qi, M.; Godt, A.; Goldfarb, D.; Han, S. G.; Sherwin, M. S. Gd(III)-Gd(III) Distances Exceeding 3 nm Determined by Very High Frequency Continuous Wave Electron Paramagnetic Resonance. *Phys. Chem. Chem. Phys.* **2017**, *19*, 5127–5136.
(22) Milikisyants, S.; Scarpelli, F.; Finiguerra, M. G.; Ubbink, M.; Huber, M. A Pulsed EPR Method to Determine Distances Between Paramagnetic Centers With Strong Spectral Anisotropy and Radicals: The Dead-Time Free RIDME Sequence. *J. Magn. Reson.* **2009**, *201*, 48–56.
(23) Dalaloyan, A.; Qi, M.; Ruthstein, S.; Vega, S.; Godt, A.; Feintuch, A.; Goldfarb, D. Gd(III)-Gd(III) EPR Distance Measurements - the Range of Accessible Distances and the Impact of Zero-Field Splitting. *Phys. Chem. Chem. Phys.* **2015**, *17*, 18464–18476.
(24) Keller, K.; Mertens, V.; Qi, M.; Nalepa, A. I.; Godt, A.; Savitsky, A.; Jeschke, G.; Yulikov, M. Computing Distance Distributions From Dipolar Evolution Data With Overtones: RIDME Spectroscopy With Gd(III)-Based Spin Labels. *Phys. Chem. Chem. Phys.* **2017**, *19*, 17856–17876.
(25) Manukovsky, N.; Feintuch, A.; Kuprov, I.; Goldfarb, D. Time Domain Simulation of Gd(III)-Gd(III) Distance Measurements by EPR. *J. Chem. Phys.* **2017**, *147*, 044201–(1–9).
(26) Jeschke, G.; Chechik, V.; Ionita, P.; Godt, A.; Zimmermann, H.; Banham, J.; Timmel, C. R.; Hilger, D.; Jung, H. DeerAnalysis2006 - A Comprehensive Software Package for Analyzing Pulsed ELDOR Data. *Appl. Magn. Reson.* **2006**, *30*, 473–498.
(27) Prokopiou, G.; Lee, M. D.; Collauto, A.; Abdelkader, E. H.; Bahrenberg, T.; Feintuch, A.; Ramirez-Cohen, M.; Clayton, J.; Swarbrick, J. D.; Graham, B.; Otting, G.; Goldfarb, D. Small Gd(III) Tags for Gd(III)-Gd(III) Distance Measurements in Proteins by EPR Spectroscopy. *Inorg. Chem.* **2018**, *57*, 5048–5059.
(28) Raitsimring, A.; Astashkin, A.; Poluektov, O.; Caravan, P. High-field Pulsed EPR and ENDOR of Gd(III) Complexes in Glassy Solutions. *Appl. Magn. Reson.* **2005**, *28*, 281–295.
(29) Potapov, A.; Song, Y.; Meade, T. J.; Goldfarb, D.; Astashkin, A. V.; Raitsimring, A. Distance Measurements in Model Bis-Gd(III) Complexes With Flexible "Bridge". Emulation of Biological Molecules Having Flexible Structure With Gd(III) Labels Attached. *J. Magn. Reson.* **2010**, *205*, 38–49.
(30) Cohen, M. R.; Frydman, V.; Milko, P.; Iron, M. A.; Abdelkader, E. H.; Lee, M. D.; Swarbrick, J. D.; Raitsimring, A.; Otting, G.; Graham, B.; Feintuch, A.; Goldfarb, D. Overcoming Artificial Broadening in Gd(III)-Gd(III) Distance Distributions Arising From Dipolar Pseudo-secular Terms in DEER Experiments. *Phys. Chem. Chem. Phys.* **2016**, *18*, 12847–12859.
(31) Doll, A.; Qi, M. A.; Wili, N.; Pribitzer, S.; Godt, A.; Jeschke, G. Gd(III)-Gd(III) Distance Measurements With Chirp Pump Pulses. *J. Magn. Reson.* **2015**, *259*, 153–162.
(32) Doll, A.; Qi, M.; Pribitzer, S.; Wili, N.; Yulikov, M.; Godt, A.; Jeschke, G. Sensitivity Enhancement by Population Transfer in Gd(III) Spin Labels. *Phys. Chem. Chem. Phys.* **2015**, *17*, 7334–7344.
(33) Bahrenberg, T.; Rosenski, Y.; Carmieli, R.; Zibzener, K.; Qi, M.; Frydrnan, V.; Godt, A.; Goldfarb, D.; Feintuch, A. Improved Sensitivity for W-Band Gd(III)-Gd(III) and Nitroxide-Nitroxide DEER Measurements With Shaped Pulses. *J. Magn. Reson.* **2017**, *283*, 1–13.
(34) Cruickshank, P. A. S.; Bolton, D. R.; Robertson, D. A.; Hunter, R. I.; Wylde, R. J.; Smith, G. M. A Kilowatt Pulsed 94 GHz Electron Paramagnetic Resonance Spectrometer With High Concentration Sensitivity, High Instantaneous Bandwidth, and Low Dead Time. *Rev. Sci. Instrum.* **2009**, *80*, 103102.
(35) Motion, C. L.; Cassidy, S. L.; Cruickshank, P. A.; Hunter, R. I.; Bolton, D. R.; Mkami, H. E.; Doorslaer, S. V.; Lovett, J. E.; Smith, G. M. The Use of Composite Pulses for Improving DEER Signal at 94 GHz. *J. Magn. Reson.* **2017**, *278*, 122 – 133.
(36) Raitsimring, A.; Astashkin, A. V.; Enemark, J. H.; Kaminker, I.; Goldfarb, D.; Walter, E. D.; Song, Y.; Meade, T. J. Optimization of Pulsed-DEER Measurements for Gd(III)-Based Labels: Choice of Operational Frequencies, Pulse Durations and Positions, and Temperature. *Appl. Magn. Reson.* **2013**, *44*, 649–670.
(37) Song, Y.; Meade, T. J.; Astashkin, A. V.; Klein, E. L.; Enemark, J. H.; Raitsimring, A. Pulsed Dipolar Spectroscopy Distance Measurements in Biomacromolecules Labeled With Gd(III) Markers. *J. Magn. Reson.* **2011**, *210*, 59–68.
(38) Jeschke, G.; Polyhach, Y. Distance Measurements on Spin-Labelled Biomacromolecules by Pulsed Electron Paramagnetic Resonance. *Phys. Chem. Chem. Phys.* **2007**, *9*, 1895–1910.
(39) Eaton, S. S.; Eaton, G. R. In *eMagRes*; Harris, R. K., Wasylishen, R. L., Eds.; American Cancer Society, 2016; pp 1543–1556.
(40) Yagi, H.; Banerjee, D.; Graham, B.; Huber, T.; Goldfarb, D.; Otting, G. Gadolinium Tagging for High-Precision Measurements of 6 nm Distances in Protein Assemblies by EPR. *J. Am. Chem. Soc.* **2011**, *133*, 10418–10421.
(41) Abdelkader, E. H.; Lee, M. D.; Feintuch, A.; Cohen, M. R.; Swarbrick, J. D.; Otting, G.; Graham, B.; Goldfarb, D. A New Gd(III) Spin Label for Gd(III)-Gd(III) Distance Measurements in Proteins Produces Narrow Distance Distributions. *J. Phys. Chem. Lett.* **2015**, *6*, 5016–5021.
(42) Yang, Y.; Yang, F.; Gong, Y. J.; Bahrenberg, T.; Feintuch, A.; ; Su, X. C.; Goldfarb, D. High Sensitivity In-Cell EPR Distance Measurements on Proteins using an Optimized Gd(III) Spin Label. *J. Phys. Chem. Lett.* **2018**, *9*, 6119–6123.
(43) Gateau, C.; Mazzanti, M.; Pecaut, J.; Dunand, F. A.; Helm, L. Solid-State and Solution Properties of the Lanthanide Complexes of a New Nonadentate Tripodal Ligand Derived From 1,4,7-triazacyclononane. *Dalton Trans.* **2003**, 2428–2433.
(44) Nocton, G.; Nonat, A.; Gateau, C.; Mazzanti, M. Water Stability and Luminescence of Lanthanide Complexes of Tripodal Ligands Derived from 1,4,7-Triazacyclononane: Pyridinecarboxamide versus Pyridinecarboxylate Donors. *Helvetica Chimica Acta* **2009**, *92*, 2257–2273.
(45) Borel, A.; Kang, H.; Gateau, C.; Mazzanti, M.; Clarkson, R. B.; Belford, R. L. Variable Temperature and EPR Frequency Study of Two Aqueous Gd(III) Complexes With Unprecedented Sharp Lines. *J. Phys. Chem. A.* **2006**, *110*, 12434–12438.
(46) Gempf, K. L.; Butler, S. J.; Funk, A. M.; Parker, D. Direct and Selective Tagging of Cysteine Residues in Peptides and Proteins With 4-nitropyridyl Lanthanide Complexes. *Chem. Commun.* **2013**, *49*, 9104–9106.
(47) Zielke, V.; Eickmeier, H.; Hideg, K.; Reuter, H.; Steinhoff, H. A Commonly Used Spin Label: S-(2,2,5,5-tetramethyl-1-oxyl-Delta 3-pyrrolin-3-ylmethyl) methanethiosulfonate. *Acta Crystallogr. C.* **2008**, *64*, o586–o589.
(48) Sanchez, J. G.; Okreglicka, K.; Chandrasekaran, V.; Welker, J. M.; Sundquist, W. I.; Pornillos, O. The Tripartite Motif Coiled-Coil is an Elongated Antiparallel Hairpin Dimer. *Proc. Natl. Acad. Sci. U.S.A.* **2014**, *111*, 2494–2499.
(49) Walton, J. W.; Bourdolle, A.; Butler, S. J.; Soulie, M.; Delbianco, M.; McMahon, B. K.; Pal, R.; Puschmann, H.; Zwier, J. M.; Lamarque, L.; Maury, O.; Andraud, C.; Parker, D. Very Bright Europium Complexes That Stain Cellular Mitochondria. *Chem. Commun.* **2013**, *49*, 1600–1602.
(50) Mason, K.; Harnden, A. C.; Patrick, C. W.; Poh, A. W. J.; Batsanov, A. S.; Suturina, E. A.; Vonci, M.; McInnes, E. J. L.; Chilton, N. F.; Parker, D. Exquisite sensitivity of the ligand field to solvation and donor polarisability in coordinatively saturated lanthanide complexes. *Chem. Commun.* **2018**, *54*, 8486–8489.
(51) Raitsimring, A.; Dalaloyan, A.; Collauto, A.; Feintuch, A.; Meade, T.; Goldfarb, D. Zero-Field Splitting Fluctuations Induced Phase Relaxation of Gd(III) in Frozen Solutions at Cryogenic Temperatures. *J. Magn. Reson.* **2014**, *248*, 71–80.
(52) Garbuio, L.; Zimmermann, K.; Haussinger, D.; Yulikov, M. Gd(III) complexes for electron-electron dipolar spectroscopy: Effects of deuteration, pH and zero field splitting. *J. Magn. Reson.* **2015**, *259*, 163–173.
(53) Ward, R.; Bowman, A.; Sozudogru, E.; El-Mkami, H.; Owen-Hughes, T.; Norman, D. G. EPR Distance Measurements in Deuterated Proteins. *J. Magn. Reson.* **2010**, *207*, 164–167.
(54) Polyhach, Y.; Bordignon, E.; Jeschke, G. Rotamer Libraries of Spin Labelled Cysteines for Protein Studies. *Phys. Chem. Chem. Phys.* **2011**, *13*, 2356–2366.
(55) Jeschke, G.; Polyhach, Y. Distance Measurements on Spin-Labelled Biomacromolecules by Pulsed Electron Paramagnetic Resonance. *Phys. Chem. Chem. Phys.* **2007**, *9*, 1895–1910.

(56) Salvadori, E.; Fung, M. W.; Hoffmann, M.; Anderson, H. L.; Kay, C. W. M. Exploiting the Symmetry of the Resonator Mode to Enhance PELDOR Sensitivity. *Appl. Magn. Reson.* **2015**, *46*, 359–368.
(57) Goldfarb, D. *Metal-Based Spin Labeling for Distance Determination. In: Timmel C., Harmer J. (eds) Structural Information from Spin-Labels and Intrinsic Paramagnetic Centres in the Biosciences. Structure and Bonding*; Springer, Berlin, Heidelberg, 2012; Vol. 152.

Graphical TOC Entry

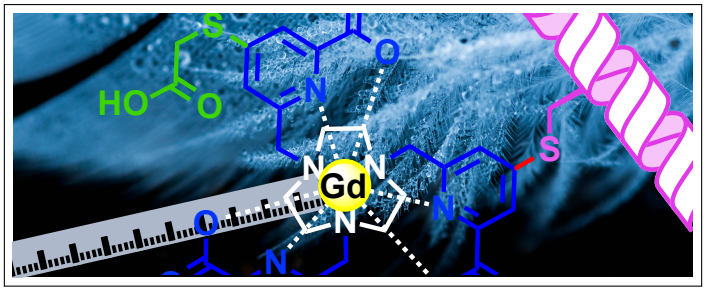

Gadolinium (III) ions have great potential as spin labels for expanding the application of EPR spectroscopy in structural biology. Here a new molecule, [Gd.sTPATCN]-SL, is synthesized, used to label the Trim25cc protein selectively at cysteine, and subsequently characterized by EPR. The label combines a short linker, narrow EPR absorption linewidth and long phase memory time. It therefore shows promise for increasing the sensitivity of distance measurements between pairs of labels with EPR.